The Extragalactic Radio Background

A. Kogut[1], D. J. Fixsen[2], S. M. Levin[3], M. Limon[4], P. M. Lubin[5], M. Seiffert[3], J. Singal[6], T. Villela[7], E. Wollack[1], and C. A. Wuensche[7]

[1] Code 665, Goddard Space Flight Center, Greenbelt, MD 20771, USA

[2] University of Maryland, Code 665, Goddard Space Flight Center, Greenbelt, MD 20771, USA

[3] Jet Propulsion Laboratory, California Institute of Technology, 4800 Oak Grove Drive, Pasadena, CA 91109, USA

[4] Columbia Astrophysics Laboratory, 550W 120th St., Mail Code 5247, New York, NY 10027-6902, USA

[5] Department of Physics, Broida Hall, Mail Code 9530, University of California, Santa Barbara, CA 93106, USA

[6] Kavli Institute for Particle Astrophysics and Cosmology, SLAC National Accelerator Laboratory, Menlo Park, CA 94025, USA

[7] Instituto Nacional de Pesquisas Espaciais (INPE), Divisão de Astrofísica, Caixa Postal 515, 12245-970 - São José dos Campos, SP, Brazil

ABSTRACT

The existence of an isotropic component of the high-latitude radio sky has been recognized for nearly fifty years, but has typically been assumed to be Galactic in origin. We use recent radio observations to test whether the observed high-latitude component could originate within either an extended Galactic halo or a more local "bubble" structure. The lack of significant polarization from the isotropic component, combined with the lack of significant correlation with the Galactic far-infrared emission, rule out an origin within the Galaxy. We conclude that an extragalactic origin is the only viable alternative for the bulk of the isotropic high-latitude emission. The extragalactic component is 2–3 times brighter than local (Galactic) emission towards the Galactic poles and is consistent with a power law in frequency with amplitude $T_r = 24.1 \pm 2.1$ K and spectral index $\beta = -2.599 \pm 0.036$ evaluated at reference frequency 310 MHz.

Key words. Galaxy: structure – radio continuum: ISM – radio continuum: general – cosmology: diffuse radiation

1. INTRODUCTION

The integrated contribution of radio continuum emission from external galaxies is expected to produce an observable background. Measurements of faint radio source counts produce a direct lower limit to the radio background, while extrapolations to still lower fluxes permit model-dependent estimates of the total source contribution. An independent measurement of the diffuse extragalactic radio flux would test the predictions from source extrapolations

to estimate the number density and radio emissivity of galaxies in the early universe, as well as details of the evolution of the radio luminosity.

A number of authors have used faint source counts to estimate the contribution of unresolved sources to the radio background, maintaining generally consistent results as surveys push to lower flux limits (Longair & Sunyaev 1972; Fomalont et al. 1984; Windhorst et al. 1993; Gervasi et al. 2008). Gervasi et al. (2008) collate surveys from 151 to 8440 MHz to fit the extragalactic source contribution to a power law,

$$T_{\rm src} = T_0 \left(\frac{\nu}{\nu_0} \right)^{\beta} \tag{1}$$

with amplitude $T_0 = 880 \pm 28$ mK antenna temperature and spectral index $\beta = -2.707 \pm 0.027$ evaluated at reference frequency $\nu_0 = 610$ MHz. A background at this intensity is large compared to the sensitivity limits of diffuse radio continuum surveys.

Observational efforts to measure the predicted extragalactic radio background have been hampered by the difficulty of clearly separating Galactic from extragalactic radio emission. Although the extragalactic component may be assumed to be isotropic, Galactic emission must be non-negative and must therefore also contain an isotropic (monopole) component. While the spectral index of individual radio sources is known, the total extragalactic background may include other sources with different spectra, so that the spectral index of the combined background is not known *a priori*. Emission from external galaxies similar to our own would produce an extragalactic background with spectrum nearly identical to the Galactic spectrum.

Turtle et al. (1962) used maps of the spectral index of the diffuse high-latitude radio continuum to estimate the amplitude of the extragalactic radio background. The results depend on the spectrum assumed for the radio background. For $\beta = -2.7$ corresponding to mean spectrum of observed populations of faint sources, the diffuse extragalactic background has amplitude $T_0 = 43 \pm 13$ K at reference frequency 178 MHz. A flatter spectrum $-2.6 < \beta < -2.4$ more typical of normal spiral galaxies at low frequencies (Rogers & Bowman 2008) would produce a larger estimate. As the extragalactic spectrum approaches the Galactic spectrum, this method becomes indeterminate, with the extragalactic temperature bounded only by the total emission towards the coldest parts of the sky, estimated as 80 ± 11 K at 178 MHz (Turtle & Baldwin 1962). Bridle (1967) uses similar techniques to yield a slightly lower estimate $T_0 = 36 \pm 7$ at 178 MHz, again for an assumed extragalactic index $\beta = -2.7$.

Spectral techniques alone can not uniquely separate an extragalactic background from a Galactic component with a similar spectrum. Phillipps et al. (1981) and Beuermann et al. (1985) used the full-sky survey at 408 MHz (Haslam et al. 1981) to construct a 3-dimensional model of Galactic emission. Both models relegate the bulk of high-latitude emission to a Galactic halo. However, the extragalactic component in these models (amplitude 6 K at 408 MHz, including the 3K cosmic microwave background) was adopted *a priori* to match estimates of radio source counts and is not the result of detailed modeling. Both larger and smaller amplitudes for the extragalactic component are compatible with these models.

Several authors estimate the radio background using indirect techniques. The continuum radio intensity in external galaxies is strongly correlated with the far-infrared intensity. If this correlation persists to higher redshift, the integrated star formation rate from redshift $z = 7$ to the present provides an estimate for the associated radio emission, ignoring the contribution from AGN or other non-thermal sources (Protheroe & Biermann 1996; Dwek & Barker 2002). The estimated contribution of 18 ± 9 K at 178 MHz provides a lower limit to the total radio background.

Kogut et al. (2011) use spatial and spectral fitting to separate high-latitude emission ($|b| > 75°$) into two components. One component is associated with the plane-parallel structure of the Galactic disk, and is clearly of Galactic origin. A second, isotropic component has a similar frequency spectrum but is not associated with commonly-used tracers of Galactic origin (csc $|b|$ spatial dependence or correlations with line emission including Hα, HI, or CII). The isotropic component is consistent with a power law from 22 MHz to 10 GHz, with amplitude $T_0 = 24.1 \pm 2.1$ K antenna temperature and spectral index $\beta = -2.559 \pm 0.036$ evaluated at reference frequency $\nu_0 = 310$ MHz to minimize covariance between the amplitude and spectral index (Fixsen et al. (2011), hereafter referred to as F11). Evaluated at 408 MHz, the isotropic conponent has amplitude 11.8 ± 1.0 K.

The isotropic component is brighter than the plane-parallel component for Galactic latitudes $|b| > 30°$, and is also brighter than estimates of the integrated emission from faint extragalactic radio sources. Based only on the spatial and frequency analysis, it can not be unambiguously assigned to either a Galactic or extragalactic origin. In this paper, we present additional tests to demonstrate that a Galactic origin for this emission violates numerous independent observations, leaving an extragalactic origin as the best remaining option.

2. Tests for Galactic Origin

The 408 MHz survey is commonly used to model Galactic synchrotron emission. The North Galactic pole has measured temperature 19 ± 3 K at 408 MHz, while a csc $|b|$ fit to the same 408 MHz map predicts a polar contribution of only 5.1 ± 0.6 K. Similar results apply to the Southern hemisphere, where the measured polar cap temperature of 21 ± 3 K significantly exceeds the value 4.0 ± 0.5 K obtained from a csc $|b|$ fit. Only 2.7 K of the difference can be attributed to emission from the cosmic microwave background, leaving a large (12 K) residual.

The existence of a bright, isotropic component of the radio sky is not new, and does not depend solely on simple csc $|b|$ models of Galactic structure. Several authors have noted the existence of this bright, isotropic component of high-latitude radio emission (Phillipps et al. 1981; Beuermann et al. 1985; Sun et al. 2008; Everett et al. 2010). Various explanations have been proposed.

2.1. Galactic Halo

Could the isotropic component originate from a Galactic halo or similar extended high-latitude structure? Previous attempts to identify emission from a Galactic halo based on

the spatial morphology of the 408 MHz survey (Phillipps et al. 1981; Beuermann et al. 1985) begin by subtracting an *a priori* estimate for the extragalactic background (typically estimated as 6 K at 408 MHz, including the cosmic microwave background), and then describe the residual signal in terms of disc and halo components. Although morphologically plausible, the resulting solution is not unique: a different choice for the extragalactic background correction would result in a different estimate for the Galactic halo contribution.

The isotropic component of the radio sky exceeds the contribution from the plane-parallel component by a factor of 2–3 at the Galactic poles. We may test models that attribute this excess to a bright radio halo by comparing these models to measurements of external galaxies. Radio observations of edge-on spiral galaxies typically show only modest high-latitude structure more typical of radio spurs extending from the disk than a true spherical halo (Hummel et al. 1991; Irwin et al. 1999, 2000). Galaxies with extended radio halos exist (NGC253, NGC4631, NGC5775, M81, M83), but in all such cases are either interacting with a close neighbor or harbor a nuclear starburst. Neither applies to the Milky Way. Even in these galaxies the extended halo component contributes much less than the emission from the disc structure (Carilli et al. 1992; Duric et al. 1998).

Hα observations of edge-on spirals indicate that atomic line emission extends into the radio halo and can be used to trace radio halo emission (Miller & Veilleux 2003). However, gas in the halo contributes only 12% of the total intensity, well short of the factor of 2–3 required to explain the observed radio excess. Kogut et al. (2011) compare the Galactic polar cap temperature derived from a plane-parallel model and the radio/CII correlation. The good agreement between the two methods can be used to limit the contribution from a halo component of the Galaxy. Comparison of the galactic component T_{Gal} obtained from the radio/CII model to that obtained from the csc $|b|$ model (which excludes any halo contribution) limits radio emission from the Galactic halo to less than $\sim$20% of the dominant plane-parallel component. While not a detection of a halo component, this upper limit is consistent with the halo contribution observed in normal edge-on spiral galaxies.

The observed level of the X-ray background places an independent limit on radio synchrotron emission from a halo extending beyond the Galactic disk. The same relativistic electrons that produce synchrotron emission by acceleration in the magnetic field will also produce X-ray emission through inverse-Compton scattering of the ambient photon fields. These photon fields include the microwave background, the infrared and optical/UV backgrounds, as well as additional infrared and optical/UV flux originating from within the Galaxy. The ratio of X-ray to synchrotron emission from a given region is determined by the relative energy density of the ambient photon fields versus the magnetic field. For fixed synchrotron emissivity, a lower magnetic field requires a higher electron Lorentz factor, which in turn increases the inverse-Compton emissivity. Radio emission from a presumed Galactic halo requires a halo magnetic field high enough to avoid over-producing the observed X-ray background.

The level of the X-ray background is known (Sreekumar et al. 1998; Gilli et al. 2007). Singal et al. (2010) estimate a lower limit to the magnetic field required to produce the observed radio excess without over-producing the X-ray background. Their calculation assumes only the intergalactic levels for the infrared and optical/UV ambient photon flux,

so it should be taken here as a strict lower limit to the magnetic field. They find that the radio excess must be produced in regions where the magnetic field exceeds 1 μG. Measurements of Faraday rotation along multiple high-latitude lines of sight limit the halo magnetic field to amplitudes below 1 μG (Taylor et al. 2009; Mao et al. 2010). A Galactic radio halo bright enough to produce the observed high-latitude excess would thus violate the observed level of diffuse X-ray emission.

2.2. Synchrotron Bubble

Could the isotropic component originate within a nearby Galactic structure? Sun et al. (2008) fit radio and microwave surveys to a three-dimensional model of Galactic synchrotron and free-free emission and conclude that the high-latitude radio excess results from a local enhancement in the density of cosmic ray electrons within approximately 600 pc of the Solar neighborhood. Evidence against a local origin comes from measurements of the polarized radio sky. Synchrotron emission from a single isotropic region with a uniform magnetic field and cosmic ray energy distribution $N(e) \propto E^{-p}$ will be linearly polarized perpendicular to the magnetic field orientation, with fractional polarization

$$f_s = \frac{p+1}{p+7/3} \tag{2}$$

(Rybicki & Lightman 1979). The frequency dependence of synchrotron emission is also related to the electron energy distribution,

$$T_A(\nu) \propto \nu^{-\beta_s} \tag{3}$$

where T_A is antenna temperature, ν is the radiation frequency, and $\beta_s = -(p+3)/2$. The observed spectral index $\beta_s = -2.6$ implies a fractional polarization as high as $f_s \sim 0.7$.

Line-of-sight and beam averaging effects will tend to reduce the observed polarization by averaging over regions with different electron energy distribution or magnetic field orientation. Sun et al. (2008) model the magnetic field and cosmic ray distribution and compare the predicted linearly polarized synchrotron emission to Wilkinson Microwave Anisotropy Probe (WMAP) observations at 23 GHz. Although their model accurately reproduces the (largely depolarized) emission from the Galactic plane, it over-predicts the observed intensity of high-latitude polarized emission by roughly a factor of 3.

Additional observational evidence against a local origin of the high-latitude excess comes from the amplitude and morphology of linearly polarized emission. In the limit that high-latitude synchrotron emission originates from a single local region centered on the Earth and pierced with a uniform magnetic field, the unpolarized emission would appear isotropic but the polarized intensity would vary as $\sin^2(\theta)$ where θ is the angle between the magnetic field and each line of sight on the sky. The isotropic component of the unpolarized intensity, scaled to 23 GHz, has amplitude 400 ± 75 μK. A local origin within a single uniform region thus predicts a distribution of polarized emission

$$P(\hat{n}) = 400 \ f_s \ \sin^2(\theta) \ \mu K \tag{4}$$

where $P = (Q^2 + U^2)^{0.5}$ is the polarized intensity, Q and U are the Stokes polarization parameters, and f_s accounts for depolarization from a turbulent component of the magnetic field along each line of sight $\hat{n}$.

WMAP observations provide a critical test for any local origin of the radio excess. Although the differential WMAP data are insensitive to a monopole component of the unpolarized intensity, the polarization maps have a well-defined zero level. WMAP data are at sufficiently high frequency that Faraday rotation is negligible, providing full-sky maps of the linear polarization to compare to the predicted distribution. We fit the seven-year WMAP 23 GHz polarization data (Jarosik et al. 2011) to the form $P(\hat{n}) = P_0 \sin^2(\theta)$, excluding from analysis the region within the P06 mask (Page et al. 2007) dominated by the Galactic plane and North Polar Spur. To avoid a positive bias from the instrument noise, we compute the cross-power

$$P^2(\hat{n}) = \frac{1}{N} \sum_{i,j} [Q_i(\hat{n})Q_j(\hat{n}) + U_i(\hat{n})U_j(\hat{n})] \tag{5}$$

for all N unique combinations of the single-year maps i and j. We compute $P(\hat{n})$ at HEALPIX resolution $N_{\mathrm{Side}} = 16$ (Górski et al. 2005), and repeatedly fit the amplitude P_0 as the symmetry axis of the $\sin^2(\theta)$ pattern is moved to each of the 3072 pixel centers. All orientations yield fitted amplitude $P_0 < 9\ \mu K$, well below the predicted value. A local origin to the high-latitude excess would thus require fractional polarization $f_s < 0.023$ for each line of sight $\hat{n}$ across the full sky. Although depolarization to this extent is observed in the Galactic plane where line-of-sight effects are severe, depolarization at high latitudes would require a ratio of turbulent to ordered magnetic field more than an order of magnitude higher than obtained by other estimates (Sun et al. 2008; Page et al. 2007; Miville-Deschênes et al. 2008).

The limit above depends on a relatively simple spatial morphology dominated by a uniform magnetic field. Polarization maps provide a comparable limit not dependent on the assumed morphology. Aside from the North Polar Spur and similar structures associated with known radio loops, the high-latitude WMAP data are strikingly faint in polarization. 50% of the WMAP 23 GHz polarization map has polarization intensity $P < 17\ \mu K$, with typical value $P \sim 10\ \mu K$. The 400 μK isotropic component identified from unpolarized radio surveys must therefore have polarization fraction $f_s \sim 0.02$ over roughly half of the sky. Depolarization to this extent would require roughly 1400 independent magnetic domains along each high-latitude line of sight, or less than 0.4 pc linear extent to a typical domain assuming a 600 pc extent for the local cosmic-ray enhancement.

Small-scale turbulence to this extent would have observational consequences. Wolleben et al. (2006) measure the linear polarization of the northern sky at 1.4 GHz. At this frequency, Faraday rotation of background polarization by a foreground screen can be appreciable. At high latitude ($|b| > 30°$), however, the polarization pattern at 1.4 GHz closely resembles that at 23 GHz, with coherent structures such as the North Polar Spur observed against a much fainter background with no evidence for additional Faraday depolarization. The lack of significant high-latitude Faraday depolarization observed in the high-latitude sky in the 1.4 GHz data argues against a nearby turbulent magnetic field. Emission from the North Polar Spur is observed to be highly polarized, with fractional polarization $f_s \sim 0.3$ at 23 GHz (Kogut et al. 2007; Miville-Deschênes et al. 2008). Since this feature lies roughly 200 pc from the Sun (Berkhuijsen 1973), high-latitude depolarization within this distance

is limited to at most a factor of 2–3, much less than the factor of 50 required to depolarize the isotropic radio excess.

2.3. Radio-Far-Infrared Correlation

Additional evidence against a Galactic origin (wherever located) comes from comparison of radio to far-infrared observations. Radio emission from external galaxies is observed to correlate tightly with the far-IR (Condon 1992). The ratio of the far-IR to radio intensity follows a linear relation

$$q = \log \left[\frac{\text{FIR}}{S_{1.4}} \right] \qquad (6)$$

where $S_{1.4}$ is the radio intensity at 1.4 GHz and the parameter

$$\text{FIR} = 1.26 \times 10^{-14} \; [2.58 f_\nu(60 \; \mu\text{m}) + f_\nu(100 \; \mu\text{m}) \,] \qquad (7)$$

captures the dominant contribution to the far-IR flux density by emission at 60 and 100 μm (Helou et al. 1985). This correlation is not simply a bolometric relation for a galaxy as a whole, but extends to detailed spatial structure on scales as small as a few hundred pc (Boulanger & Perault 1988; Murphy et al. 2006) to perhaps 50 pc (Hughes et al. 2006; Tabatabaei et al. 2007).

Assuming that emission from our Galaxy follows this relation, we may use observations of Galactic far-IR emission to infer the associated high-latitude radio emission. We take the absolute COBE/DIRBE maps at 60 and 100 μm and subtract the contributions from Solar System zodiacal emission (Kelsall et al. 1998) and the cosmic infrared background (Fixsen et al. 1998) to obtain full sky maps of the Galactic component of far-IR emission. Applying the mean FIR/radio ratio $\langle q \rangle = 2.3 \pm 0.2$ observed for local normal galaxies (Condon 1992) to the absolute intensity of Galactic FIR emission yields estimated radio brightness temperature 145 ± 85 mK for the polar cap at 1.4 GHz, nearly identical to the 147 ± 10 mK derived from cosecant fit (Kogut et al. 2011). Alternatively, we may compare the spatial structure of the 1420 MHz survey to the Galactic FIR emission map to derive the local FIR/radio correlation, and apply this local correlation to the FIR intensity measured at the polar cap to obtain an estimate of the Galactic radio brightness 117 ± 35 mK at the polar cap, independent of measurements in external galaxies.

The ratio of FIR to radio emission within the Galaxy is consistent with the mean value observed for local normal galaxies (Boulanger & Perault 1988), and yields a value for the associated high-latitude Galactic radio emission consistent with that obtained by a simple plane-parallel model or correlations with other tracers of Galactic emission. The observed high-latitude emission is much brighter. Attributing the isotropic component of the high-latitude emission to a Galactic origin would thus require either that Galactic emission depart from the nearly universal FIR/radio correlation observed in external galaxies, or that the emission originate in nearby structures smaller than the 50–200 pc scale typical of the FIR/radio correlation. As noted above, the observed depolarization of the high-latitude excess rules out a nearby origin.

2.4. Geomagnetic Origin

Relativistic electrons trapped in the Earth's magnetic field emit synchrotron radiation (Dyce et al. 1959). This emission is both strongly polarized and anisotropic, with intensity peaking near the Earth's magnetic equator and falling to zero at the poles. It is measured to be less than 3 K at 30 MHz and expected to be much less than 1 mK at 3 GHz (Ochs et al. 1963; Peterson & Hower 1963). It therefore is unable to explain the observed high-latitude excess.

3. Discussion

It is difficult to reconcile the observed bright, isotropic high-latitude emission with an origin within the Galaxy. Attributing the bulk of the high-latitude radio intensity to a Galactic origin would require either that the Galaxy be markedly unusual in several different properties compared to normal spiral galaxies (e.g. unusually large halo, unusual FIR/radio correlation, and unusual X-ray emissivity) or that the nearby magnetic field is both markedly unusual in its ratio of the turbulent to regular components and highly anisotropic (patchy) so that large-scale polarized features such as the North Polar Spur are viewed immediately adjacent to broad depolarized regions.

In contrast, assigning an extragalactic origin to the isotropic component produces a single consistent model with no discrepancies between the inferred Galactic properties and those of typical spiral galaxies. Estimates of the Galactic contribution based solely on the $\csc |b|$ spatial morphology agree with observations of external spiral galaxies as well as with independent estimates of Galactic radio emission based only on the correlation of radio intensity with tracers known to be of Galactic origin (atomic line emission or Galactic far-IR intensity). The results do not vary significantly as additional tracers are fit simultaneously. The ratio of the Galactic far-IR intensity to the Galactic component of radio intensity agrees with the FIR/radio correlation observed in external galaxies.

Assigning an extragalactic origin to the isotropic component eliminates the problem of anomalously low polarization fraction observed in the high-latitude WMAP data. Although the WMAP data provides a well-determined map of the polarized intensity $P(\hat{n})$, the fractional polarization f_s depends on the absolute intensity of the unpolarized synchrotron emission and is therefore uncertain. We use a simple model of the synchrotron intensity to investigate the range of f_s in the high-latitude sky. We take the 408 MHz survey and subtract the 2.725 K CMB monopole and the WMAP maximum-entropy map of free-free emission (Gold et al. 2011) to obtain a map dominated by synchrotron emission $I(\hat{n})$. We then scale the synchrotron map to 23 GHz using a spatially invariant spectral index $\beta = -2.6$, and compute the fractional polarization $f_s = P(\hat{n})/I(\hat{n})$ for pixels within the faintest 50% of the polarization map $P(\hat{n})$. If the isotropic component of high-latitude radio emission is Galactic in origin, the synchrotron intensity $I(\hat{n})$ must contain this component. The resulting fractional polarization has mean $\langle f_s \rangle = 0.02$. If instead the isotropic component is extragalactic, we assume it is unpolarized and subtract it from the Galactic synchrotron map $I(\hat{n})$ to re-compute the fractional polarization. The resulting decrease in the unpolarized synchrotron intensity increases the derived fractional polarization to
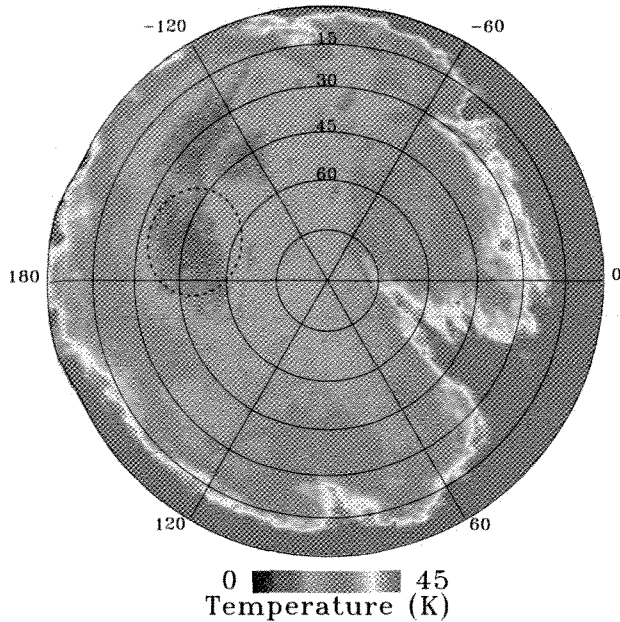
Fig. 1. The northern Galactic hemisphere of the 408 MHz survey shows an extended cold region above the Galactic anti-center (dashed line). The coldest regions are consistent with minimal anisotropic Galactic emission superposed on an isotropic background.

$\langle f_s \rangle = 0.14$, much closer to the value $0.2 < f_s < 0.3$ observed toward bright local features such as North Polar Spur where contribution of the isotropic component is much smaller (Kogut et al. 2007; Miville-Deschênes et al. 2008).

The exact value of the fractional polarization depends on the spectral index used to scale the galactic (anisotropic) component of the 408 MHz survey; a steeper index or spectral break would further reduce the estimated unpolarized synchrotron intensity $I(\hat{n})$ at 23 GHz and thereby further increase f_s. In all cases, however, an extragalactic origin for the isotropic component increases the derived f_s and reduces the requirement for extensive depolarization along every high-latitude line of sight.

One possible objection to an extragalactic origin is that the F11 power-law fit is in some tension with the observed temperature towards the coldest region of the sky. A cursory comparison of the power-law radio background to individual full-sky radio surveys shows that some pixels in some surveys are colder than the best-fit radio background. Does this falsify an extragalactic origin to the high-latitude radio excess? Figure 1 shows the northern Galactic hemisphere of the 408 MHz survey. The visual impression of the coldest high-latitude emission regions is a diffuse Galactic cirrus overlaying an isotropic component. Figure 2 shows a histogram of the sky temperatures from the coldest region of the 408 MHz map, above the Galactic anti-center at $(l, b) = (196°, \; 48°)$. The coldest observed temperature values are well described by a Gaussian distribution of standard deviation

0.64 K centered at mean temperature 13.55 K, with additional shoulders or secondary peaks at higher temperatures. Based solely on the histogram, the coldest region of the 408 MHz survey is consistent with the superposition of a uniform component (either Galactic or extragalactic) at temperature 13.55 K observed with effective noise 0.64 K per pixel, plus an additional 2–3 K of anisotropic Galactic emission. The noise term inferred from the Gaussian width is consistent with the 1 K estimate quoted for the total noise (including systematic effects) in the 408 MHz map (Haslam et al. 1981). The coldest pixels in this region are consistent with downward noise fluctuations in the radio sky brightness and are not a direct constraint on the mean background intensity.

The background intensity inferred from the histogram of pixel temperatures agrees well with the background derived from 2-dimensional models of Galactic emission (Kogut et al. 2011). The coldest region of the 408 MHz survey is consistent with temperature 13.55 ± 0.64 K, of which an undetermined portion is extragalactic, plus 2–3 K of additional Galactic emisssion (Figure 2). Modeling this region using either the csc $|b|$ or CII techniques from Kogut et al. (2011) yields estimates of 11.3 ± 1.8 K for the total background (including the CMB) and 2.9 ± 0.5 K for the Galactic component, in excellent agreement with the values inferred from the histogram alone. Estimates for the extragalactic background derived from modeling the 408 MHz data at the North or South Galactic poles are slightly higher (although still in statistical agreement), and result in a mean value of 14.1 ± 3.4 for the total extragalactic background derived solely from the 408 MHz data. This value includes both the CMB and any extragalactic radio background and is consistent with the measured sky temperature in this region within the respective uncertainties.

A similar comparison can be made for other radio surveys. Surveys at 22 MHz (Roger et al. 1999), 45 MHz (Maeda et al. 1999; Alvarez et al. 1997), 408 MHz (Haslam et al. 1981), and 1420 MHz (Reich et al. 2001; Reich & Reich 1986) have full or nearly-full sky coverage at frequencies where Galactic radio emission is significant. Figure 3 shows a histogram of the full-sky temperature distribution for each of these surveys. As with Fig
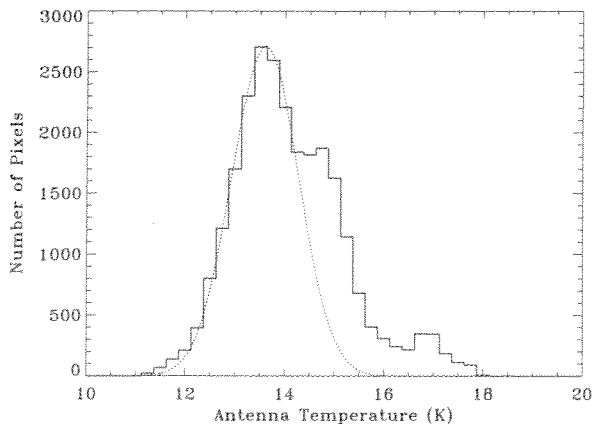

Fig. 2. Histogram of pixel temperatures from the coldest patch in the 408 MHz survey (dashed region in Figure 1). The dotted line shows a Gaussian fit with mean temperature 13.55 K and width 0.65 K.
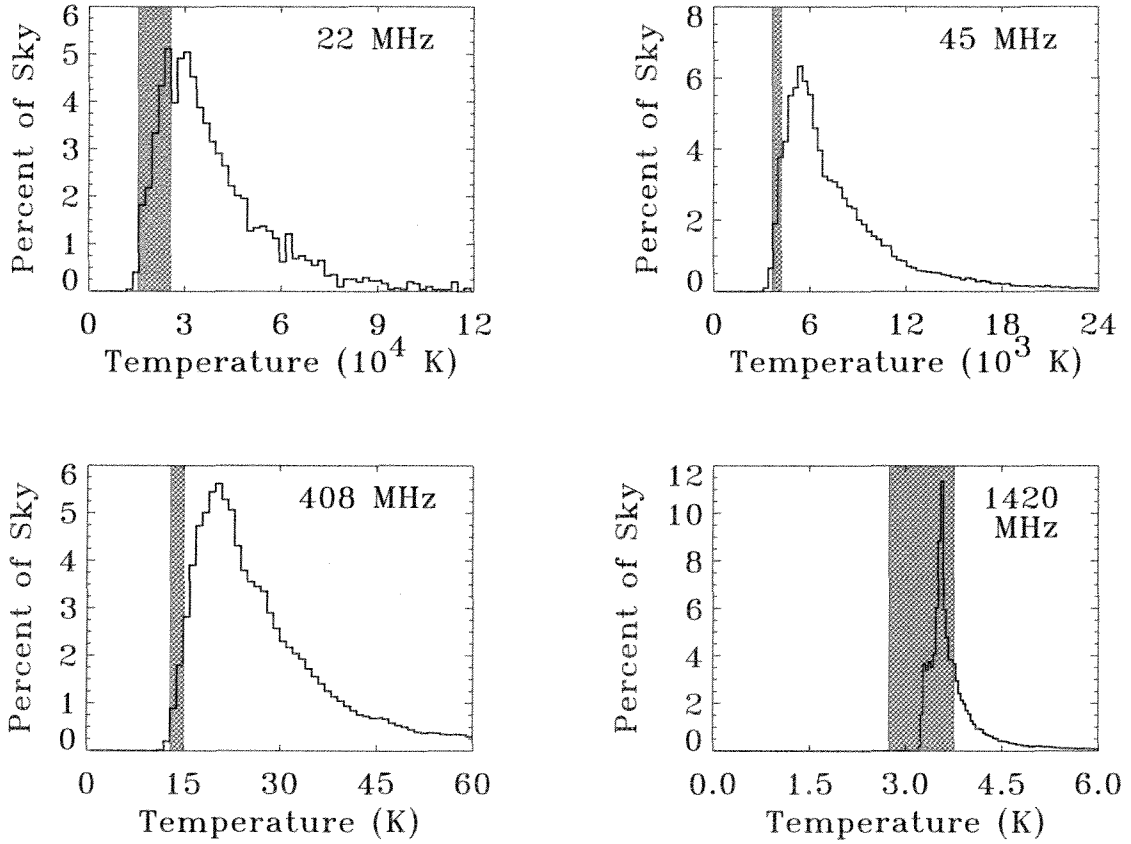
Fig. 3. Histogram of pixel temperatures over the full sky for low-frequency radio surveys. The gray bars indicate the estimated background temperature $\pm$ 1 σ at each frequency.

2, the high temperature side of the distribution shows a long tail indicating regions of variable emission. As before, merely selecting the coldest single pixel in each map biases the background estimate downward, since noise fluctuations can lower as well as raise the temperature estimate for an individual pixel. A true background would generate a sharp edge on the lower side of the distribution, which would then be slightly blurred by noise. Figure 3 shows the histograms of the low frequency sky maps, along with our estimates of the background temperature and uncertainty derived from the Galactic modeling of each individual map. All four estimates of the background derived from Galactic modeling (grey bands in Fig 3) hug the low temperature edge of the distributions. Only a few pixels (less than 1%) appear more than one standard deviation below our background estimate. This is to be expected if the noise in a single pixel is comparable to or larger than the background uncertainty derived from Galactic modeling.

Downward noise fluctuations prevent use of the coldest few pixels as a direct limit on a possible background component. However, the coldest sky *patch* is in fact a broad minimum on the sky containing many independent pixels. The amplitude of the power-law fit for the excess emission exceeds the mean temperature of this broad minimum for some of the sky maps used in this analysis. For example, the 22 MHz survey has a broad minimum near

Table 1. Antenna Temperature In Coldest Sky Patch

Frequency	Temperature	Galaxy	CMB	Residual	F11 Model
(MHz)	(K)	(K)	(K)	(K)	(K)
22	17300 ± 5100	3900 ± 500	3	13400 ± 5100	23300 ± 2900
45	3680 ± 440	770 ± 120	3	2910 ± 460	3630 ± 400
408	14.2 ± 1.7	2.9 ± 0.5	2.7	8.6 ± 1.8	11.8 ± 1.0
1420	3.28 ± 0.53	0.11 ± 0.02	2.72	0.45 ± 0.53	0.46 ± 0.05

17300 K, while the power-law model of Fixsen et al. (2011), evaluated at 22 MHz, predicts a radio background of 23300 K. Does this falsify a claimed extragalactic background? Several points must be considered. The first is that both the measured sky temperature and the predicted model amplitude have non-trivial uncertainties. Including uncertainties, the comparison is thus between the measured sky temperature 17300 ± 5100 K and the model prediction 23300 ± 2900 K, which differ by only one standard deviation. Nevertheless, the model prediction does exceed the sky temperature, while the sky temperature must contain at least some Galactic contribution. Does this invalidate the model? Table 1 compares the measured sky temperature to the Galactic emission model in the coldest patch of the sky. Each map shows a positive residual after subtracting the CMB and modeled Galactic emission from the measured temperature of the coldest sky patch. Fitting these residuals to a power law

$$T = T_r \left(\frac{\nu}{\nu_0} \right)^{\beta} \tag{8}$$

yields amplitude $T_r = 18 \pm 3$ K and spectral index $\beta = -2.59 \pm 0.09$ at reference frequency $\nu_0 = 310$ MHz. The residuals from the coldest sky patch follow the same spectral index as the F11 model, but with amplitude smaller by $\sim 25\%$.

The F11 model uses data from the coldest patch, but includes additional data from the North and South Galactic poles where model uncertainties are smaller. This model extracts 3 parameters (CMB temperature, radio amplitude and radio spectral index) from 60 individual estimates of the extragalactic background derived from 2 Galactic model techniques evaluated along 3 lines of sight at 10 observing frequencies. Each of these 60 individual estimates yields a positive residual after subtracting the Galactic contribution, including all 6 estimates derived solely from 22 MHz data. The F11 model combines the resulting background estimates at different frequencies and different lines of sight to yield a single radio amplitude and spectral index. We assume that the errors in each estimate follow a Gaussian distribution and propagate them through the full 60×60 covariance matrix as described in Fixsen et al. (2011). The difference between the individual estimates and the best-fit model should then in turn follow a normal distribution, with some input estimates lying above the best-fit model and some lying below. In practice, the 45 MHz and 1420 MHz input estimates lie above the best-fit model while the 22 MHz and 408 MHz data lie below. Since the χ^2 of resulting solution is acceptable (17.4 for 11 degrees of freedom), we conclude that the distribution of points both above and below the mean is consistent with the expected result of combining multiple measurements into a few-parameter model, with

all residuals well within the gain and offset uncertainties of the individual low-frequency sky maps.

Data from the coldest regions of the 4 low-frequency radio surveys yields a smaller amplitude T_r than the F11 model, which includes additional lines of sight and additional surveys where uncertainties in both the Galactic model and survey zero level are smaller. Although the smaller amplitude from the lowest-frequency surveys could indicate a more complicated spectral dependence, adding additional parameters to account for a possible spectral break or curvature is not statistically justified. Alternatively, we could adjust the power-law model for a one-sided fit in which the model is bounded to remain at or below the individual input values but not allowed to exceed the central value of any input estimate. Given the substantial zero-level uncertainties of the various low-frequency radio surveys, such a one-sided fit would produce a biased estimate of the radio background. Since all of the 60 input values yield non-zero estimates for the extragalactic background and the power-law model yields an acceptable χ^2 value, we conclude that parameterized model provides an adequate statistical description of the multi-frequency sky data.

Comparison of the modeled extragalactic component to the total emission in the coldest regions of the radio sky suffers from the relatively large uncertainty in the absolute level of existing low-frequency radio surveys. At frequencies 3–10 GHz, the well-calibrated ARCADE 2 data show a clear residual well in excess of the beam spillover to the ground (Fixsen et al. 2011). At lower frequencies, both calibration uncertainty and ground pickup become appreciable. The amplitude of the modeled extragalactic component becomes comparable to the ground temperature (250 – 300 K) at frequencies near 120 MHz. A sky survey at this frequency would thus minimize the uncertainty from ground radiation in the antenna sidelobes to better constrain the frequency dependence of emission from the faintest regions of the sky.

4. Conclusions

The existence of an isotropic component of the high-latitude radio sky has been recognized for nearly fifty years, but has typically been assumed to be Galactic in origin. We adopt the power-law parameterization presented in Fixsen et al. (2011) and critically examine the hypothesis of a Galactic origin. Any Galactic origin would require our Galaxy to be unusual in one or more aspects compared to typical spiral galaxies. An origin within a galactic halo or similar structure with radius large compared to 7 kpc would require the Galactic radio halo to exceed the brightness of typical edge-on spiral galaxies by a factor of 30. A handful of galaxies with true extended halos have been observed, but even these halos are too faint by a factor of 10 to explain the observed high-latitude excess. In addition, cosmic ray electrons capable of producing the observed diffuse synchrotron emission within an extended Galactic halo must also produce a diffuse X-ray background by Compton scattering the diffuse photon field within the halo. Simultaneously satisfying the observed synchrotron emission while not over-producing an X-ray background would require a halo magnetic field of 1 μG or larger, in violation of the limit derived from the rotation measure observed along high latitude lines of sight.

An origin within a more local bubble (with the solar system near the center) could evade these constraints, but would generate appreciable linear polarization, which is not observed. Multiple independent magnetic domains along each line of sight could in principle depolarize emission from a local structure, but the resulting ratio of turbulent to ordered magnetic field exceeds previous estimates by at least an order of magnitude. In addition, observation of significant fractional polarization within known Galactic structures such as the North Polar Spur show that any significant depolarization must occur at distances larger than the distance to such structures.

Any origin of the observed synchrotron excess within the Galaxy would require the Galaxy to deviate markedly from the ratio of radio to far-infrared emission observed in external galaxies. The ratio of radio to far-IR emission within the Galaxy, derived from spatial fluctuations in the two components, agrees well with the mean value observed in external galaxies, and yields a value for the associated high-latitude Galactic radio emission consistent with that obtained by a simple plane-parallel model or correlations with other tracers of Galactic emission. The observed high-latitude emission is much brighter. Attributing the observed high-latitude emission to a Galactic origin would thus require either that Galactic emission responsible for the isotropic excess depart from the nearly universal FIR/radio correlation observed in external galaxies, or that the excess emission originate in nearby structures smaller than the 50–200 pc scale typical of the FIR/radio correlation. As noted above, the observed depolarization of the high-latitude excess rules out a nearby origin.

Placing the observed isotropic component within the Galaxy violates multiple independent astrophyical observations, leaving an extragalactic origin as the only remaining option. Assigning an extragalactic origin to the isotropic component obviates the need for the Galaxy to differ from typical spiral galaxies. The ratio of disk to halo emission as well as the ratio of Galactic far-IR to radio emission are then near the mean observed for local normal spirals. An extragalactic origin also eliminates the need for extensive synchrotron depolarization along high-latitude lines of sight. We conclude that the isotropic component is extragalactic in origin.

The origin of the extragalactic radio background is unknown. Although the observed spectral index is clearly indicative of synchrotron emission, the amplitude is more than twice as large as the estimated contribution from known populations of faint radio sources (Gervasi et al. 2008). To explain the observed radio background without over-producing the far-infrared background, the source of the radio background must be radio-bright compared to the radio/far-IR ratio observed in faint radio galaxies. Seiffert et al. (2011) and Singal et al. (2010) compare the F11 model to extrapolated source populations to conclude that a new population of faint radio sources would be required to explain the observed radio excess.

References

Alvarez, H., Aparici, J., May, J., & Olmos, F. 1997, A&AS, 124, 315

Berkhuijsen, E. M. 1973, A&A, 24, 143

Beuermann, K., Kanbach, G., & Berkhuijsen, E. M. 1985, A&A, 153, 17

Boulanger, F. & Perault, M. 1988, ApJ, 330, 964

Bridle, A. H. 1967, MNRAS, 136, 219

Carilli, C. L., Holdaway, M. A., Ho, P. T. P., & de Pree, C. G. 1992, ApJ, 399, L59

Condon, J. J. 1992, ARA&A, 30, 575

Duric, N., Irwin, J., & Bloemen, H. 1998, A&A, 331, 428

Dwek, E. & Barker, M. K. 2002, ApJ, 575, 7

Dyce, R. B., Dolphin, L. T., Leadabrand, R. L., & Long, R. A. 1959, J. Geophys. Res., 64, 1815

Everett, J. E., Schiller, Q. G., & Zweibel, E. G. 2010, ApJ, 711, 13

Fixsen, D. J., Dwek, E., Mather, J. C., Bennett, C. L., & Shafer, R. A. 1998, ApJ, 508, 123

Fixsen, D. J., Kogut, A., Levin, S., et al. 2011, ApJ, in press

Fomalont, E. B., Kellermann, K. I., & Wall, J. V. 1984, ApJ, 277, L23

Gervasi, M., Tartari, A., Zannoni, M., Boella, G., & Sironi, G. 2008, ApJ, 682, 223

Gilli, R., Comastri, A., & Hasinger, G. 2007, A&A, 463, 79

Gold, B., Odegard, N., Weiland, J. L., et al. 2011, ApJS, 192, 15

Górski, K. M., Hivon, E., Banday, A. J., et al. 2005, ApJ, 622, 759

Haslam, C. G. T., Klein, U., Salter, C. J., et al. 1981, A&A, 100, 209

Helou, G., Soifer, B. T., & Rowan-Robinson, M. 1985, ApJ, 298, L7

Hughes, A., Wong, T., Ekers, R., et al. 2006, MNRAS, 370, 363

Hummel, E., Beck, R., & Dettmar, R. 1991, A&AS, 87, 309

Irwin, J. A., English, J., & Sorathia, B. 1999, AJ, 117, 2102

Irwin, J. A., Saikia, D. J., & English, J. 2000, AJ, 119, 1592

Jarosik, N., Bennett, C. L., Dunkley, J., et al. 2011, ApJS, 192, 14

Kelsall, T., Weiland, J. L., Franz, B. A., et al. 1998, ApJ, 508, 44

Kogut, A., Dunkley, J., Bennett, C. L., et al. 2007, ApJ, 665, 355

Kogut, A., Fixsen, D. J., Levin, S. M., et al. 2011, ApJ, in press

Longair, M. S. & Sunyaev, R. A. 1972, Soviet Physics Uspekhi, 14, 569

Maeda, K., Alvarez, H., Aparici, J., May, J., & Reich, P. 1999, A&AS, 140, 145

Mao, S. A., Gaensler, B. M., Haverkorn, M., et al. 2010, ApJ, 714, 1170

Miller, S. T. & Veilleux, S. 2003, ApJS, 148, 383

Miville-Deschênes, M., Ysard, N., Lavabre, A., et al. 2008, A&A, 490, 1093

Murphy, E. J., Braun, R., Helou, G., et al. 2006, ApJ, 638, 157

Ochs, G. R., Farley, Jr., D. T., Bowles, K. L., & Bandyopadhyay, P. 1963, J. Geophys. Res., 68, 701

Page, L., Hinshaw, G., Komatsu, E., et al. 2007, ApJS, 170, 335

Peterson, A. M. & Hower, G. L. 1963, J. Geophys. Res., 68, 723

Phillipps, S., Kearsey, S., Osborne, J. L., Haslam, C. G. T., & Stoffel, H. 1981, A&A, 103, 405

Protheroe, R. J. & Biermann, P. L. 1996, Astroparticle Physics, 6, 45

Reich, P. & Reich, W. 1986, A&AS, 63, 205

Reich, P., Testori, J. C., & Reich, W. 2001, A&A, 376, 861

Roger, R. S., Costain, C. H., Landecker, T. L., & Swerdlyk, C. M. 1999, A&AS, 137, 7

Rogers, A. E. E. & Bowman, J. D. 2008, AJ, 136, 641

Rybicki, G. B. & Lightman, A. P. 1979, Radiative processes in astrophysics, ed. Rybicki, G. B. & Lightman, A. P.

Seiffert, M., Fixsen, D. J., Kogut, A., et al. 2011, ApJ, in press

Singal, J., Stawarz, L., Lawrence, A., & Petrosian, V. 2010, MNRAS, 409, 1172

Sreekumar, P., Bertsch, D. L., Dingus, B. L., et al. 1998, ApJ, 494, 523

Sun, X. H., Reich, W., Waelkens, A., & Enßlin, T. A. 2008, A&A, 477, 573

Tabatabaei, F. S., Beck, R., Krause, M., et al. 2007, A&A, 466, 509

Taylor, A. R., Stil, J. M., & Sunstrum, C. 2009, ApJ, 702, 1230

Turtle, A. J. & Baldwin, J. E. 1962, MNRAS, 124, 459

Turtle, A. J., Pugh, J. F., Kenderdine, S., & Pauliny-Toth, I. I. K. 1962, MNRAS, 124, 297

Windhorst, R. A., Fomalont, E. B., Partridge, R. B., & Lowenthal, J. D. 1993, ApJ, 405, 498

Wolleben, M., Landecker, T. L., Reich, W., & Wielebinski, R. 2006, A&A, 448, 411